CERN-ACC-2020-0027
original : 26-08-2020
last update: 14-01-2021
androula.alekou@cern.ch

Report

Design of a Fast Single-turn Extraction for the ESSnuSB Accumulator

A. Alekou[1, 2], H. Bartosik[1], I. Efthymiopoulos[1]*
[1]CERN, Switzerland, [2]Uppsala University

Abstract

In the European Spallation Source (ESS) neutrino Super Beam (ESSnuSB), a very intense neutrino beam will be produced in order to measure with a high precision the CP violating angle at the 2nd oscillation maximum. An accumulator ring is included in the ESSnuSB design that allows converting a series of linac pulses to single intense pulses that subsequently will bombard the neutrino production targets. This report presents the conceptual design for a one-turn fast extraction ejecting the proton beam from the ESSnuSB accumulator ring towards the beam transport channel to the neutrino targets.

Keywords: ESS, ESSnuSB, fast extraction, accumulator, neutrinos.

[*]Work supported by ESSnuSB Design Study, EU Consortium Agreement 77419

Contents

1 Introduction

The European Spallation Source (ESS), which is currently under construction in Lund, Sweden, will be the world's highest brightness neutron source [1]. In its present state, ESS is powered by a 5 MW proton linac that can be further modified to provide an additional 2.5 GeV, 5 MW of beam power of H^- beam to feed a third generation intense neutrino Super Beam (ESSnuSB) facility. ESSnuSB is a Long-Baseline neutrino oscillation experiment using a megaton-scale Water Cherenkov detector located in underground mines at 540 or 360 km from the neutrino source. ESSnuSB aims at measuring with a high precision the CP violating angle at the 2nd oscillation maximum [2] and resolve the neutrino mass hierarchy problem.

The layout of ESSnuSB Facility is shown in Figure 1. The extracted beam from the LINAC is directed via a beam transfer channel to the accumulator ring. The accumulator has as principal role to compress the long pulses from the LINAC to single intense beam pulses that are fast extracted and arrive via a beam transport channel to the four targets where the neutrino source is produced. This pulse compression is mandatory principally for two reasons: a) to overcome the thermal power limitations from the pulsing of the secondary particle focusing device (the magnetic horns) that operate at high current and b) to help reducing the background from atmospheric neutrinos (and other sources) to the far detectors by gating to the beam pulses.

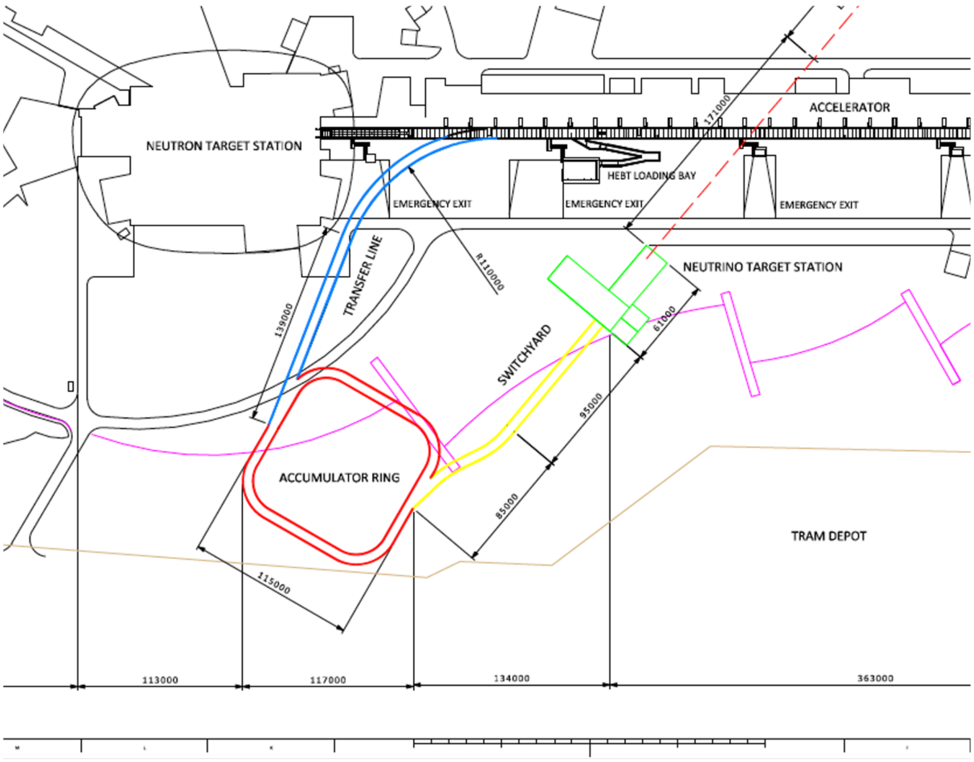

Fig. 1: Layout of the ESSnusB facility.

To overcome the limitations in the neutrino production target technology to sustain beam pulses beyond the range of 1-1.5 MW of power [3], a novel concept using four identical target systems is adopted: four targets are used, each one receiving successively a compressed pulse from the accumulator of max 1.6 MW of power. The baseline pulsing scheme for the accumulator is shown in Figure 2. The short linac pulses are successively grouped to form mid and then macro-pulses at a frequency of 14Hz. Each macro-pulse consists of four mid-pulses of 650 μs spaced by 100 μs together for a duration of 2.9 ms. Each of the mid-pulses corresponds to a cycle of the accumulator that is filled with 490 LINAC pulses, each of 1.29 μs, spaced by 100 ns.

The accumulator ring is shown in Figure 3. It has four straight sections, each focusing on the beam injection, collimation system for beam halo scraping, extraction, and RF cavities for longitudinal beam shaping. The ring circumference is 384.01 m, with the injected beam filling 90% of the ring, leaving approximately 133 ns for the extraction gap. A barrier-bucked RF scheme is used to maintain

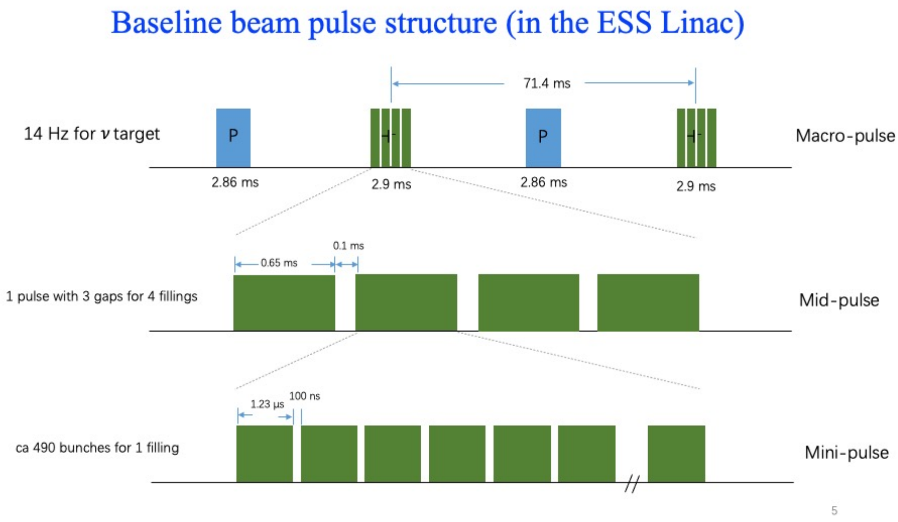

Fig. 2: The baseline pulsing scheme for ESSnuSB.

the extraction gap clean. The beam is fast-extracted from Straight Section 3 (SS3) in a single turn. This report presents the conceptual design of the one-turn proton extraction, optics designs and h/w design specifications.

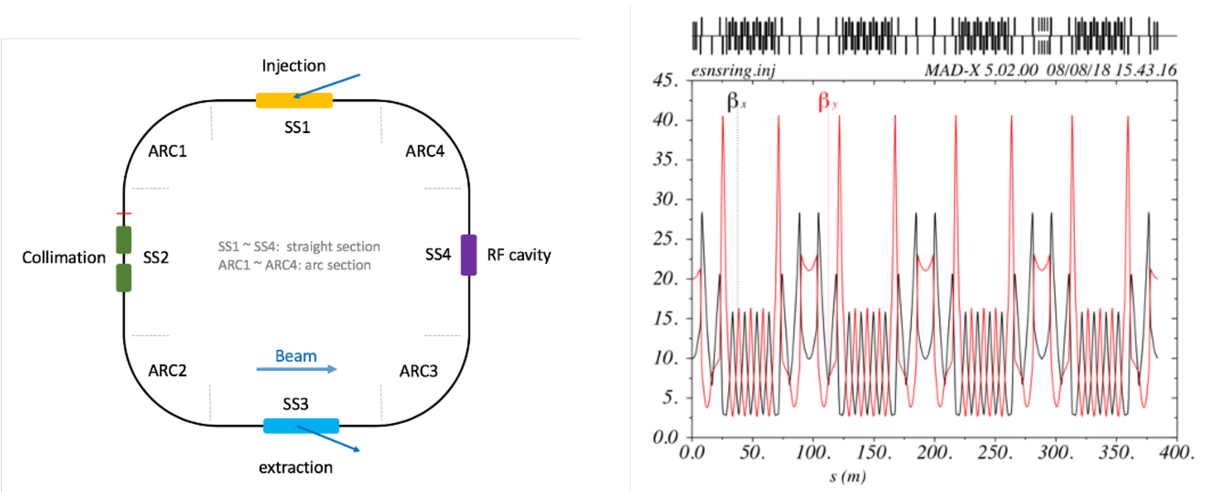

Fig. 3: ESSnuSB accumulator schematic (left) and betatron functions (right). [4]

A summary of the ESSnuSB parameters can be found in Table 1.

2 The fast extraction

Once filled, the intense beam from the accumulator should be fast extracted to the beam transfer line towards the neutrino production targets, creating a ≈1.5 MW short pulse of 1.23 μs. Figure 4 illustrates the layout for a fast extraction scheme. In a typical implementation, a set of slow (∼ms) bumpers, installed in a drift cell of the ring lattice, introduce a bump to the closed orbit such to bring it closer to an extraction septum. Then a fast kicker deflects the beam which is further deflected by a quadrupole that is defocusing in the extraction plane such that it passes the blade of the septum. The septum then further deviates the beam in the extraction or the opposite plane towards the extraction channel. The "3-corrector" slow orbit bump shown in the figure, brings the circulating beam closer to the septum thus helping to reduce the strength of the fast kicker. The fast kicker deflects the entire beam into the septum in a single turn.

For the case of the ESSnuSB accumulator, such a scheme cannot be directly implemented. This

Table 1: ESSnuSB parameters summary

Parameter	Unit	Value
Circumference	[m]	384.01
Average beam power	[MW]	5
Injection/Extraction Kinetic energy	[GeV]	2.5
Beam momentum	[GeV/c]	3.308
Pulse average current	[mA]	50
Pulse duration from linac	[ms]	3.5
Pulse repetition rate	[Hz]	14
Filling time	[μs]	650
Time between fills	[μs]	100
Beam intensity per filling		2.2×10^{14}

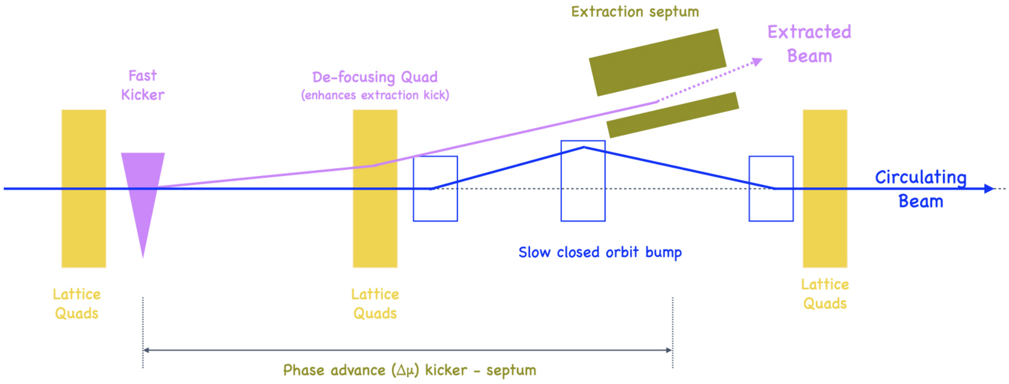

Fig. 4: Schematic view of a fast extraction layout. [5]

because, first, the accumulator is not cycled and in the baseline filling scheme as described above is constantly filled and emptied. Thus the closed orbit (CO) bump would have to be fixed, which in turn can be equivalent to optimizing the layout and apertures of the extraction section, bringing the septum to the closest possible position to the CO. In an alternative filling scheme where the LINAC mid-pulses could be spaced further apart, considered as one possible option in the ESSnuSB, such a scheme could be envisaged. Secondly, in the standard lattice of the machine the quadrupoles of the SS come in doubled pairs (focusing-defocusing) thus there is no direct gain for the extraction trajectory. A modified lattice layout separating the quad-doublets is under evaluation. Thus, for the case of the ESSnuSB accumulator a simple layout is proposed and studied: a set of four kickers around the central quadrupole doubled in SS3 is used to extract in a single turn the beam to the septum as shown in Figure 5.

Such a scheme was successfully implemented for the SNS facility in USA and the proton beam extraction from their accumulator ring. In their implementation the proton extraction from the accumulator, employs a total of 14 fast kickers to deflect the accumulated 1.3 GeV beam to the septum and beam tranfer line to the spallatin target (see Figure 6).

2.1 Design considerations

Figure 7 shows the accumulator ring lattice layout for the straight sections SS2 ("standard") and SS3 ("extraction"). Inspired by the SNS design, we adopted the concept of a vertical downwards extraction with the kickers, and a large horizontal deflection out of the ring with the septum. In our case as seen in Figure 1, the extracted beam needs to be kicked in a large downward angle to arrive at the target hall, as well as horizontally in order to correctly point to the far neutrino detectors, so there is no need to have the septum tilted. For the septum, we considered the same deflection angle as for SNS, i.e. **16.8 deg** [7], that gives a beam separation of approx. 50 cm at the exit of a 3 m long magnet (or ~1.6 m from its rotation point) with a field of 1.0 T for our beam momenta. This means we can place the septum at

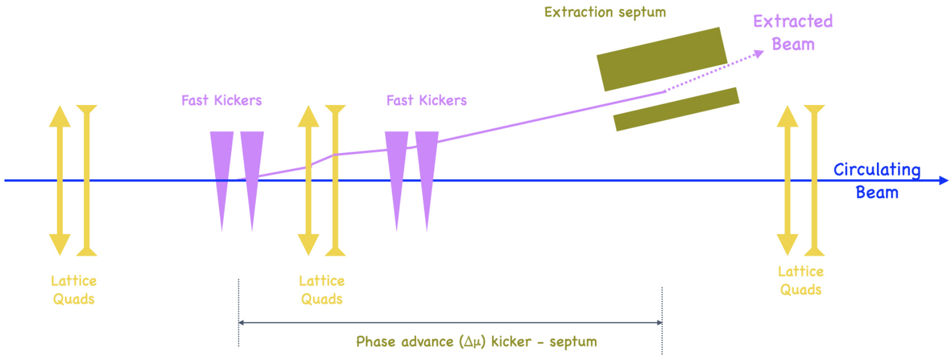

Fig. 5: Schematic view of the ESSnuSB accumulator fast extraction layout.

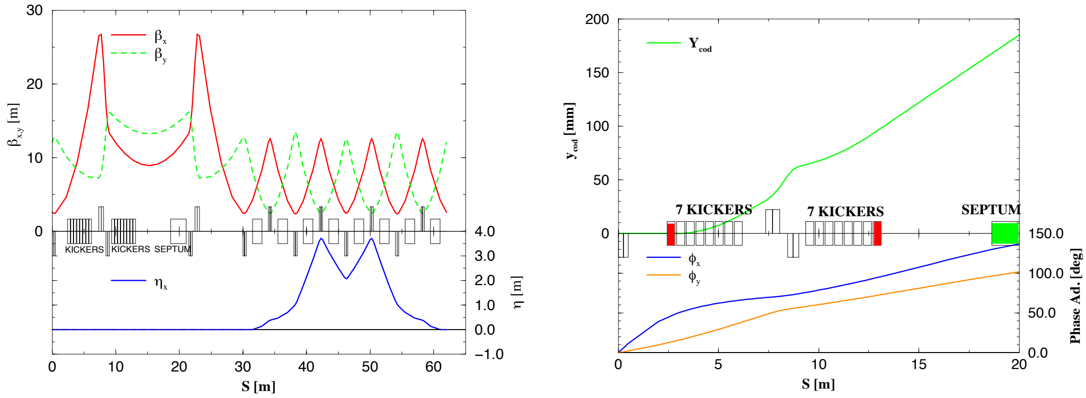

Fig. 6: Optics (left) and layout (right) of SNS ring extraction. The beam is kicked vertically by 14 kickers and extracted horizontally by a Lambertson septum. [6]

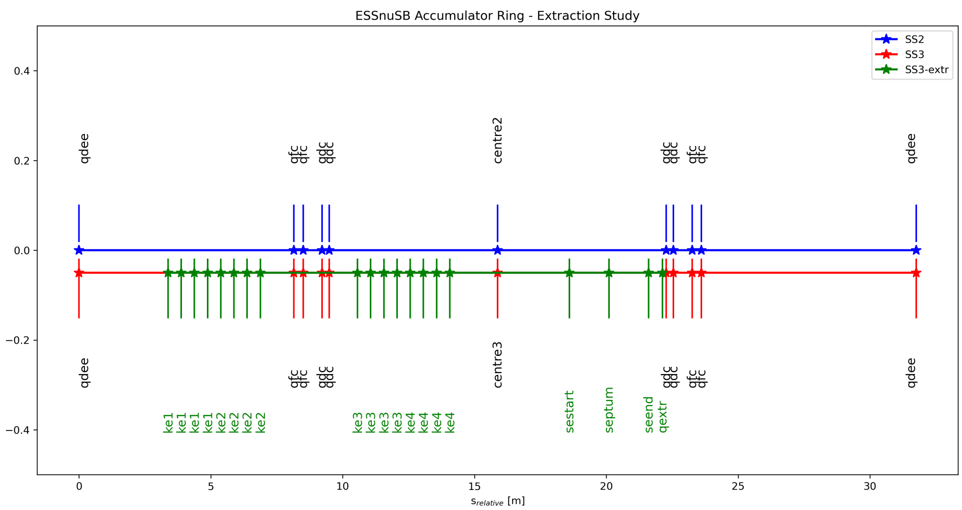

Fig. 7: Accumulator ring lattice layout for straight sections SS2 ("standard"), and SS3 ("extraction"). For SS3 the lattice elements, identical to SS2 assuring the four-fold symmetry of the accumulator, are shown in red. The added extraction elements are indicated in green.

minimal distance to the lattice quadrupoles, thus leaving the full SS space for placing the kickers.

Figure 8 shows the circulating beam envelop in the SS3 region, estimated using 180 $\pi \mathrm{mm} \cdot \mathrm{mrad}$ as full beam acceptance. This value is explicitly chosen to be larger than the acceptance of the secondary collimators that define the maximum beam envelop in order to have a safety margin in the design (see Table 2). In addition, we considered a safety margin of 1 cm when calculating the aperture values for

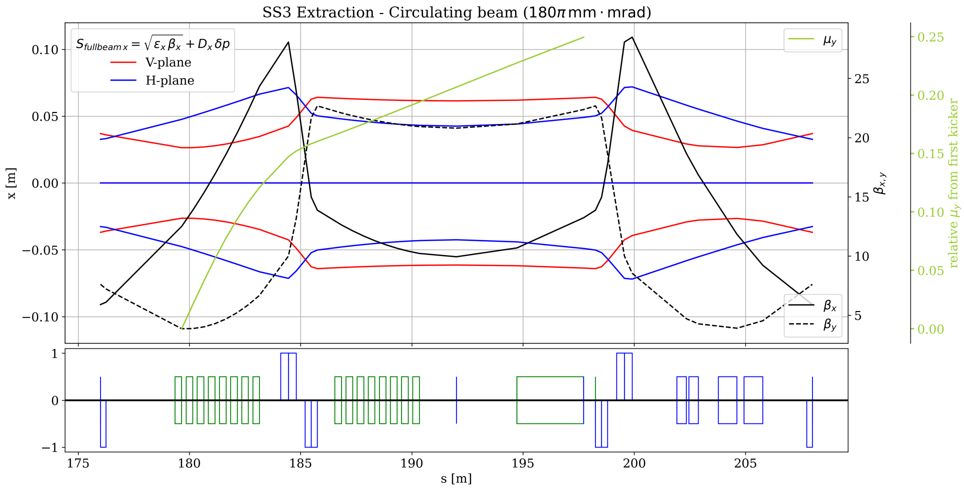

Fig. 8: The full beam envelop for the circulating beam in SS3 region. The betatron values and the relative vertical phase advance from the first kicker magnet to the septum is also shown.

Table 2: Accumulator ring full beam acceptance emittance values.

Element	100% geometrical emittance [π mm.mrad]
Primary collimator	70
Secondary collimator	120
Circulating beam vacuum chamber and elements	200
SS3 and extraction elements	180

the extraction elements. For a y-position of the closed orbit at the entrance of the septum, the kicker vertical deflection, θ_y, is determined as :

$$\theta_y = \frac{y}{\sqrt{\beta_{y,k}\beta_{k,s}}\ \sin\mu_y} \tag{1}$$

where $\beta_{y,k}$ and $\beta_{y,s}$ are the vertical beta functions at the location of the kicker and septum respectively, and μ_y is the phase-advance between them. In order to require the smallest deflection kicker-angle, the phase-advance between the kicker and septum should be aimed to be close to $(2n+1)\cdot\pi/2$, where n is an integer; in addition, the septum should be placed as far away from the kicker as possible. Further, in order to reduce the kicker strength, and minimize the impact of an element failure, a larger number of shorter kickers is considered.

In the proposed configuration, sixteen kickers grouped by four and placed around the central quadrupole doubled of SS3 are used, followed by a Lambertson septum magnet placed just upstream the following quadrupole doublet.

2.2 Implementation and parameters

The configuration of the septum is schematically shown in Figure 9. The strength of the kickers is determined such to deflect the extracted beam from the closed orbit to the center of the field region in the extraction septum. As illustrated in Fig. 9, the vertical distance y_{extr} is calculated as:

$$\begin{aligned} y_{\text{extr}} &= \sigma_{\text{circ}} + y_{\text{aperture margin}} + \text{septum blade width} + y_{\text{aperture margin}} + \sigma_{\text{extr}} \\ &= \text{septum half aperture}_{\text{circ beam}} + \text{septum blade width} + y_{\text{aperture margin}} + \sigma_{\text{extr}} \end{aligned}$$

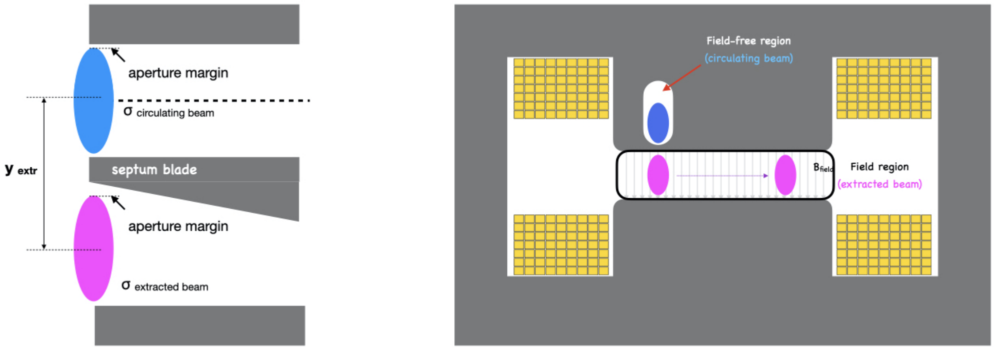

Fig. 9: Schematic view of the septum. Left: side view at the upstream end, Right: cross-section view.

with $\sigma_{\text{circ}}, \sigma_{\text{extr}}$ are the full beam width of the circulating and extracted beam at the entrance of the septum, estimated from the optics functions:

$$\sigma_{\text{circ, extr}} = \sqrt{\beta_{\text{entr}} \cdot J_{\text{septum}}} + \delta p/p \cdot \Delta_y, \tag{2}$$

where $\beta_{\text{entr}}, J_{\text{septum}}$ are the beta-function at the entrance of the septum, and the septum's acceptance of the circulating and extracted beams respectively. For a septum blade of 10 mm, and an aperture margin of **10 mm**, y_{extr} is found to be -161.0 mm.

Table 3: Optics functions of the extraction elements. The phase-advance difference, $\Delta\mu_y$, is between the centre of each element and the septum centre.

name	s [m]	x [mm]	y [mm]	β_x [m]	β_y [m]	μ_x [2π]	μ_y [2π]	$\Delta\mu_y$ [2π]
ke1:1	179.506	0.0	-0.1	12.1125	3.881	3.978	3.942	0.245
ke1:2	180.006	0.0	-0.9	13.4451	3.855	3.984	3.963	0.224
ke1:3	180.506	0.0	-2.4	14.8864	3.959	3.990	3.983	0.204
ke1:4	181.006	0.0	-4.7	16.4364	4.193	3.995	4.003	0.184
ke2:1	181.506	0.0	-7.8	18.0951	4.557	3.999	4.021	0.166
ke2:2	182.006	0.0	-11.6	19.8625	5.051	4.004	4.038	0.150
ke2:3	182.506	0.0	-16.0	21.7387	5.674	4.007	4.052	0.135
ke2:4	183.006	0.0	-21.2	23.7236	6.428	4.011	4.066	0.122
ke3:1	186.692	0.0	-70.3	12.7793	22.152	4.042	4.115	0.072
ke3:2	187.192	0.0	-72.6	12.2696	21.909	4.048	4.119	0.068
ke3:3	187.692	0.0	-75.6	11.8103	21.689	4.055	4.122	0.065
ke3:4	188.192	0.0	-79.3	11.4012	21.494	4.062	4.126	0.061
ke4:1	188.692	0.0	-83.6	11.0425	21.322	4.069	4.130	0.057
ke4:2	189.192	0.0	-88.5	10.7341	21.175	4.076	4.134	0.054
ke4:3	189.692	0.0	-94.0	10.4760	21.052	4.084	4.137	0.050
ke4:4	190.192	0.0	-100.1	10.2682	20.952	4.091	4.141	0.046
septum start:1	194.728	0.0	-161.0	10.6819	21.150	4.163	4.176	0.011
septum center:1	196.228	-1.3	-177.6	11.9670	20.736	4.184	4.187	0.000
septum end:1	197.728	0.6	-194.3	13.1815	20.542	4.203	4.199	-0.012

Each of the 16 kickers has a length of 0.3 m. In order to simplify their design and ease the installation and maintenance, they are grouped by four with the elements in the group having the same aperture and strength. Since the aperture of the kickers is expected to increase towards the extraction to accommodate for the beam deflection, their strength was scaled accordingly. This choice was made aiming to achieve the same overall design difficulty. With this in mind, using MAD-X [8], the strength of the kickers was matched to the desired y_{extr}-coordinate for the extracted beam at the entrance of the septum as defined above. Table 3 provides the vertical optics functions at the center of the extraction elements. The optics functions at the entrance of the first quadrupole of the extraction line placed 2 m from the end of the extraction septum are given in Table 4.

Table 4: Basic optics variables at the septum and first quad of the transfer line to the target (R2S).

Variable	units	septum entry	septum center	septum exit	Quad- R2S line
s	[m]	194.728	196.228	197.728	199.903
β_x	[m]	10.682	11.967	13.181	16.143
β_y	[m]	21.150	20.736	20.542	19.384
D_x	[m]	0.048	-0.064	-0.406	-1.073
D_y	[m]	0.107	0.102	0.096	0.066
μ_x	[2π]	4.163	4.184	4.203	4.226
μ_y	[2π]	4.176	4.187	4.199	4.216

The apertures of all the elements in the extraction section were calculated such to contain the full beam envelop including a margin of 1 cm. This is to include possible variations of the kicker field during extraction or single element failures. Table 5 gives the apertures of the elements in SS3. Figure 10

element	horizontal aperture [mm] [mm]	vertical apreture [mm]
sep -circ	[-59.038, 59.038]	[-73.693, 73.693]
sep -extr (entry)	[-500.000, 59.038]	[-83.693, -233.189]
sep -extr (exit)	-	[-118.221, -265.581]
qfc	[-81.916, 81.917]	[-106.586, 58.876]
qdc	[-66.897, 66.897]	[-141.720, 80.021]
qde	[-43.192, 43.192]	[-48.680, 48.680]

Table 5: Calculated apertures for the extraction section elements.

shows the circulating and extracted beam orbit and envelop. The 16 kickers are shown in groups of four, the Lambertson septum is illustrated in magenta, whereas the lattice quadrupoles are shown in brown. The strengths of each kicker group as well as the magnetic field is summarized in Table 6.

Table 6: Kicker design parameters.

Group	Multiplicity	Aperture-H [mm]	Aperture-V [mm]	Length [m]	Angle [mrad]	B-field [mT]	BL [mT.m]
ke1	4	$\pm$65.41	[-43.42, 37.85]	0.30	-1.540	-56.62	-16.987
ke2	4	$\pm$76.48	[-67.76, 44.79]	0.30	-1.386	-50.96	-15.289
ke3	4	$\pm$57.90	[-153.13, 73.28]	0.30	-1.338	-49.20	-14.759
ke4	4	$\pm$54.62	[-173.93, 72.12]	0.30	-1.204	-44.28	-13.283
				Total angle	-21.87 [mrad], -1.253 [deg]		

As described in Section 2, the kicker should be able to deflect the circulating beam within the foreseen extraction gap of max. 130 ns. In Figure 11 the specifications for the kicker pulse are described. In the present design of the accumulator ring, the barrier bucket implementation assures minimal leakage of particles in the extraction gap of 133 ns [9], from which we can assume that no particles are expected in the gap of 120 ns. Thus we define as baseline parameters for the kicker rise time R(2-98%) in 100 ns, reaching a stable current in the designed value of 120 ns. The kicker pulse should remain for the whole duration of the turn, i.e. 1.5-1.6 μs and then ramp down within 100 μs to be ready for the next cycle.

The above specifications of the kickers can serve in a second phase as input to an engineering study for their construction, possibly including some optimisation R&D. We note that kickers of similar parameters have been constructed for SNS [10] and the CERN PS Booster extraction [11].

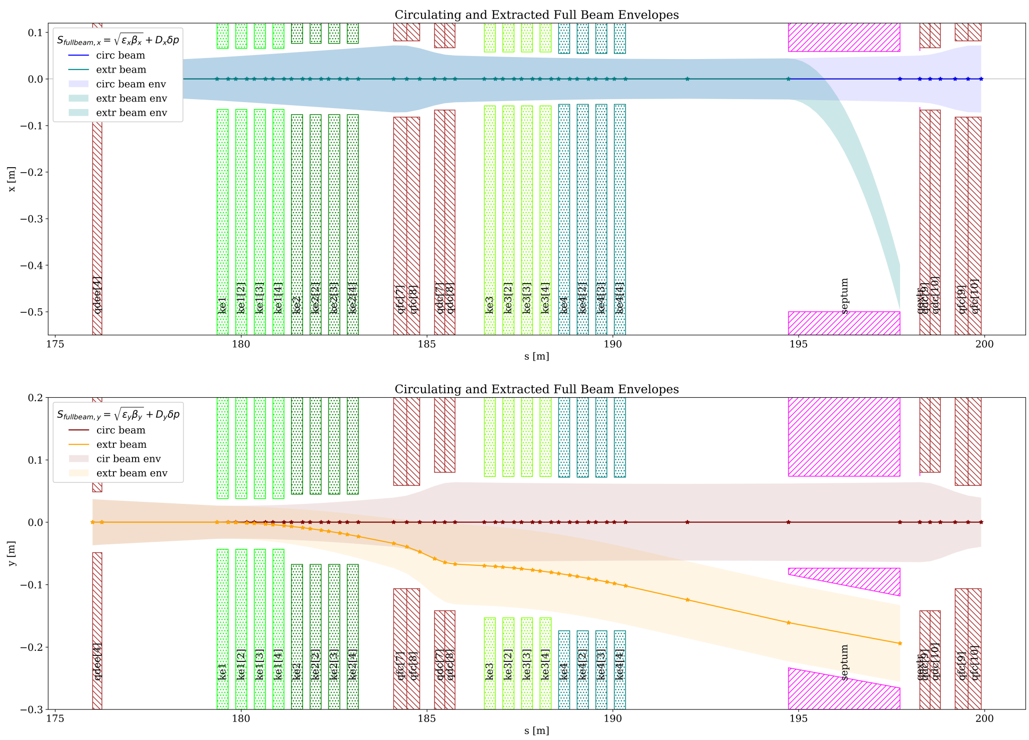

Fig. 10: The circulating and extracted beam trajectories and beam envelops (100% acceptance). The four kicker groups are indicated in variants of green.

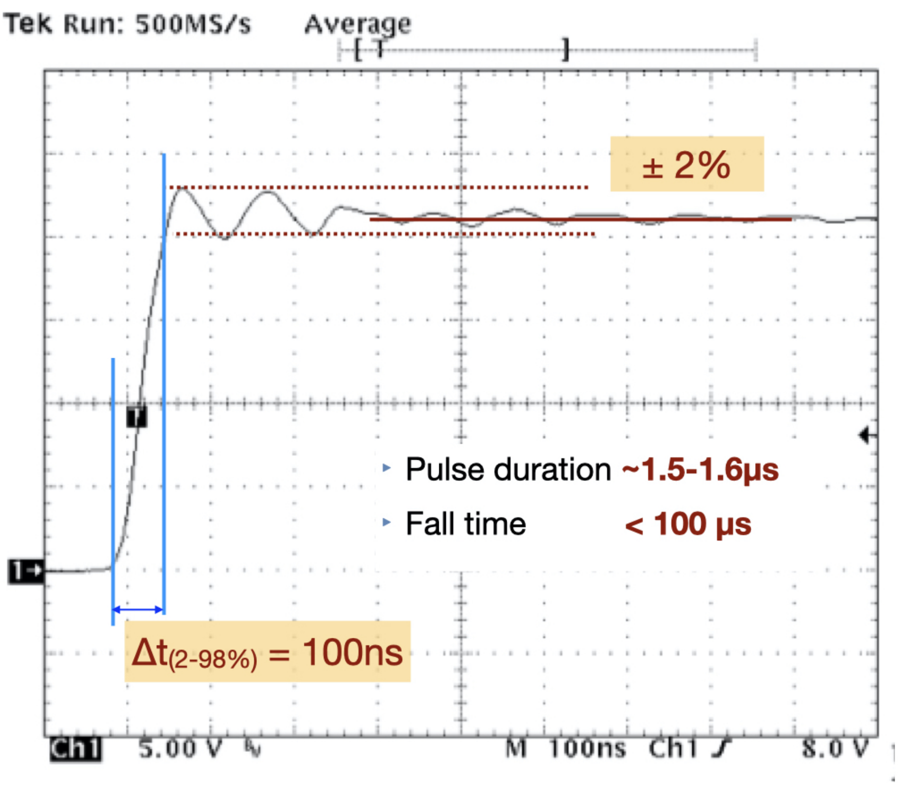

Fig. 11: Fast kicker pulse specifications.

2.2.1 Failure scenarios

Since the accumulated beam will be of high-power reaching 1.6 MW, accounting for possible failures already in the design phase is imperative. Two cases are studied: a) a $\pm 2\%$ variation in the kicker field,

b) single element failure in the sixteen kicker assembly. The first case simulates a possible uncorrected ripple in the kicker field strength as explained above until it is stabilised to the nominal value. To be on the safe-side, the error is assigned in all sixteen kickers, where in a real implementation it can be compensated automatically among the four power supplies. The resulting beam trajectories and envelop is shown in Figure 12. As can be seen, the chosen apertures are sufficient to provide sufficient clearance and avoid losses even in this pessimistic case.

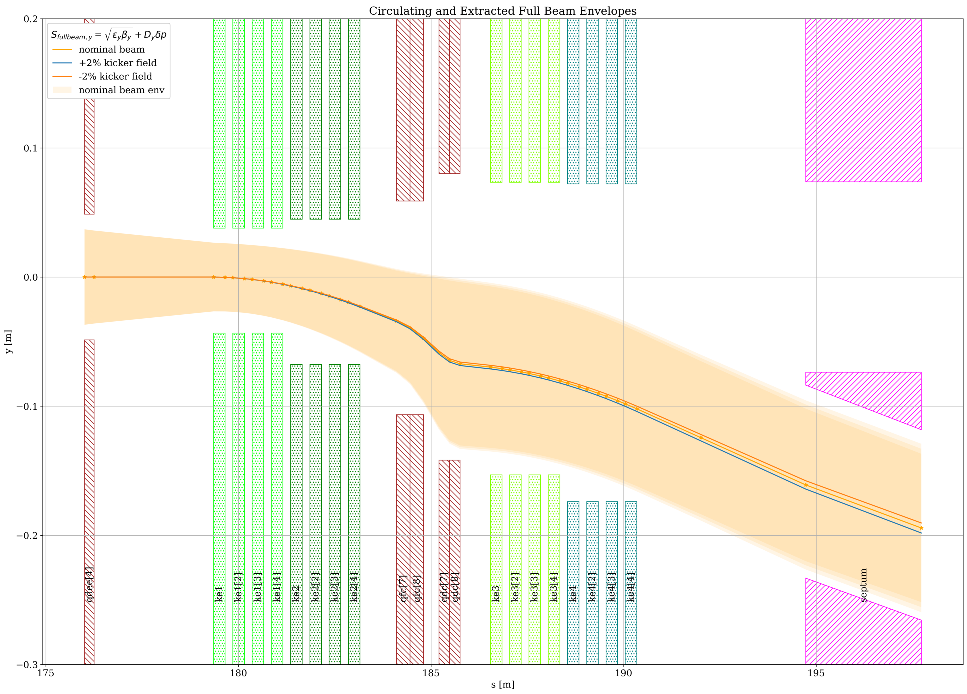

Fig. 12: Effect on the extracted beam trajectory for $\pm 2\%$ error in the kicker strength.

To study the second case, we switched off, using MAD-X simulations, the strength of one single kicker at a time. The resulting trajectories and beam envelops are shown in Figure 13. Also in this case, the chosen apertures provide sufficient margin for the beam to pass without losses. For both cases, the resulting orbit variations need to be followed in the beam transfer line up to the target.

3 Conclusions

This report presented the optics design for a one-turn fast extraction ejecting the proton beam from the accumulator into the extraction beam transfer line to the neutrino target. Following the design constraints, a proposed implementation using sixteen kickers and a Lambertson septum is explained. The strengths and apertures of the extraction elements including the sixteen fast kickers and the Lambertson septum are provided. All magnet designs are within the limit of normal-conductivity, and of similar value to what is available in operation in present facilities. The chosen apertures seem robust to the basic possible error or failure cases that are also studied.

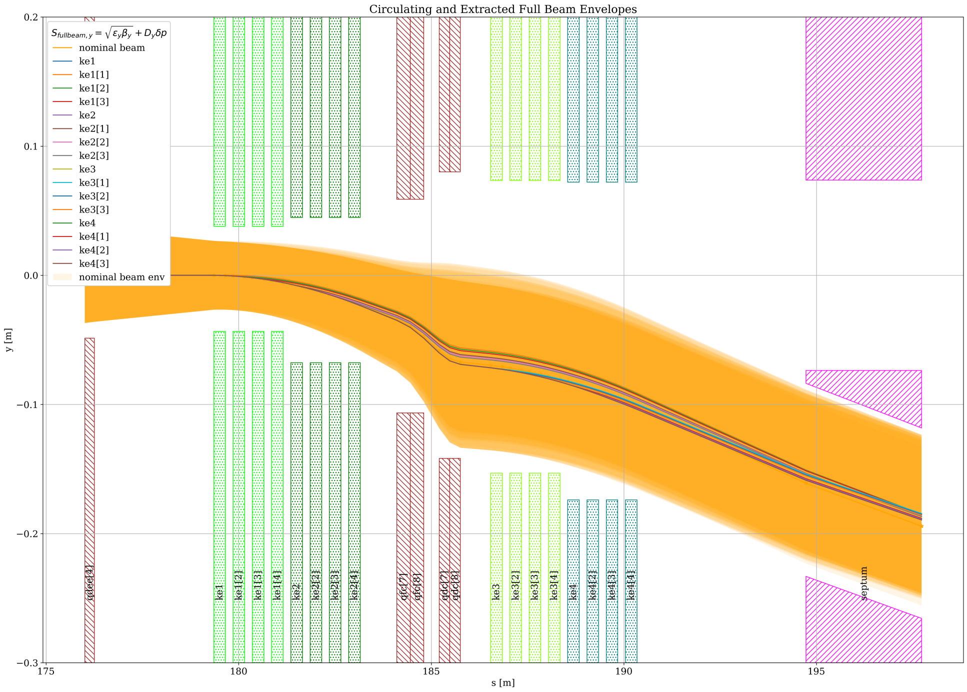

Fig. 13: Effect of a single kicker failure to the extracted beam trajectory.

4 References

[1] S. Peggs. ESS Technical Design Report. Technical Report ESS-DOC-274, Lund, 2013.

[2] Elena Wildner et al. The Opportunity Offered by the ESSnuSB Project to Exploit the Larger Leptonic CP Violation Signal at the Second Oscillation Maximum and the Requirements of This Project on the ESS Accelerator Complex. *Adv. High Energy Phys.*, 2016:8640493, 2016.

[3] E. Baussan et al. Neutrino super beam based on a superconducting proton linac. *Phys. Rev. ST Accel. Beams*, 17:031001, 2014.

[4] Ye Zou, Elian Bouquerel, Marcos Dracos, Tord Ekelöf, Mohammad Eshraqi, Björn Gålnander, Maja Olvegård, Roger Ruber, Horst Schönauer, and Elena Wildner. Status of the ESSnuSB accumulator design. In *10th International Particle Accelerator Conference*, page MOPRB046, 2019.

[5] M A Fraser. Fast extraction: single and multi-turn. *CERN Yellow Rep. School Proc.*, 5:285. 29 p, 2018.

[6] D. Raparia. SNS injection and extraction devices. *Conf. Proc. C*, 0505161:553, 2005.

[7] N. Gazis. Near Detector location & layout at the ESS site, 2019.

[8] H. Roy G. Schmidt F. Deniau, L. Grote et al. MADX. Available at `http://mad.web.cern.ch/mad/`.

[9] Ye Zou. The accumulator ring for the ESSnuSB project - a progress report. *PoS*, NuFact2019:061, 2020.

[10] N. Tsoupas, M. Blaskiewicz, Y.Y. Lee, J.L. Mi, A. Soukas, J.G. Wang, J. Wei, and S.Y. Zhang. Beam extraction from the SNS ring and design of extraction kickers. *Conf. Proc. C*, 0006262:2270–2272, 2000.

[11] K D Metzmacher and L Sermeus. The PSB Ejection and Recombination Kicker Systems for LHC. Technical Report CERN-PS-CA-Note-2000-004, CERN, Geneva, 2000.